MedChemComm

Accepted Manuscript

This is an *Accepted Manuscript*, which has been through the Royal Society of Chemistry peer review process and has been accepted for publication.

Accepted Manuscripts are published online shortly after acceptance, before technical editing, formatting and proof reading. Using this free service, authors can make their results available to the community, in citable form, before we publish the edited article. We will replace this *Accepted Manuscript* with the edited and formatted *Advance Article* as soon as it is available.

You can find more information about *Accepted Manuscripts* in the Information for Authors.

Please note that technical editing may introduce minor changes to the text and/or graphics, which may alter content. The journal's standard Terms & Conditions and the Ethical guidelines still apply. In no event shall the Royal Society of Chemistry be held responsible for any errors or omissions in this *Accepted Manuscript* or any consequences arising from the use of any information it contains.

ROYAL SOCIETY OF CHEMISTRY

www.rsc.org/medchemcomm

Synthesis of sliver nanoparticles loaded sulfadiazine/polyvinyl alcohol nanorods and their antibacterial activities

Ping Li[b], Xiangmin Xu[c], Longlong Wu[b], Binjie Li[a*], YanbaoZhao[b]

Sliver nanoparticles loaded sulfadiazine/polyvinyl alcohol nanorods (Ag-SD/PVA NRs) were successfully synthesized in an ammonia solution, which were characterized by XRD, FT-IR, SEM and TEM. In the process, PVA was introduced to control the size of silver sulfadiazine (SSD) precursor and further reduce SSD to produce Ag-SD/PVA NRs. The obtained Ag-SD/PVA NRs have average width of 50 nm and length of 300 nm, loaded with Ag NPs about 8 nm in size. As novel composite antibacterial agents, Ag-SD/PVA NRs exhibited higher bactericidal efficacy in comparison with that of Ag NPs and SSD microrods (MRs) alone. Additionally, these Ag-SD/PVA NRs showed concentration-dependent antibacterial behavior. At high concentration, they displayed more effective antibacterial activity towards *S. aureus* than *P. aeruginosa* and *E. coli*, and at lower concentrations they exhibited more effective towards *E. coli*.

1. Introduction

Since the increasing microbial infection events occur, there are growing attentions in the development of new and effective antibacterial agents.[1-4] It is well known that silver-based compounds are widely used in antibacterial materials because of their high antibacterial activity and broad antibacterial spectrum.[5,6] For example, silver sulfadiazine (SSD) is used in burn therapy. Here, silver ions provide the primary antibacterial activity against a range of bacteria and fungi, while sulfadiazine (SD) has bacteriostatic properties.[7] However, the antibacterial activity of SSD would always be discounted for its low solubility resulted in a slow release of silver ions. Therefore, many researches are focusing on improving the solubility and antibacterial efficacy of SSD by forming composite nanoparticles .[8]

In all inorganic antibacterial agents, silver nanoparticles (Ag NPs) have been extensively studied due to their high antibacterial activity with minimal perturbation to human cells, but their practical applications are often hampered by the ease of aggregation, which would decrease their antibacterial properties. To solve this problem,

[a] *Medical School of Henan University, Kaifeng 475004, P. R. China. E-mail: lbj821@163.com .*

[b] *Key Laboratory for Special Functional Materials, Henan University, Kaifeng 475004, P. R. China*

[c] *Yellow River Conservancy Technical Institute, Kaifeng 475004, P. R. China*

different organic materials such as polymers,[9] quaternary ammonium compounds,[10] and antimicrobial peptides,[11] have been employed to stabilize Ag NPs and endow them long-term synergistic antibacterial performance.

Here, we designed and fabricated novel antibacterial agents, sliver nanoparticles loaded sulfadiazine/polyvinyl alcohol nanorods (Ag-SD/PVA NRs). The nanosized SD/PVA composites possess the excellent solubility in the aqueous solution, and provide organic matrix to increase the stability of the Ag NPs, which combine the antibacterial activities of SD and Ag NPs for the excellent performance of the product. To the best our knowledge, the corresponding complex and structure haven't been reported in literatures.

2 Results and discussion

2.1 Chemistry

In a typical procedure: 0.225 g of PVA, 0.500 g of SD and 100 mL of diluted ammonia (2 wt%) were added into a flask and mixed with ultrasonic agitation to form a clear solution. Then, 2 mL of $AgNO_3$ solution (1 M) was dropwised into the solution at room temperature with constant magnetic stirring. The colorless solution was gradually changed to white, and subsequently to light grey suspension. After reacting for 4 h, the grey precipitation was separated by centrifugation and washed with excess amount of ethanol at least 3 times. Finally, the powder was obtained by vacuum drying at ambient temperature. As comparative materials, Ag NPs and SSD microrods (MRs) were obtained via similar procedures without addition of SD and PVA, respectively.

2.2 Characterization of Ag-SD/PVA NRs

The typical XRD pattern of Ag-SD/PVA NRs is given in Fig. 1a. In the pattern, the peaks at scattering angles 2θ of 7.1°, 11.7°, 12.8°, 14.1°, 16.5°, 19.7°, 20.9°, 21.3°, 23.8°, 26.0°, 27.4° and 28.7° are attributed to the crystal planes of (001), (-201), (200), (002), (011), (-210), (012), (003), (-402), (400), (212) and (004) of monoclinic SD

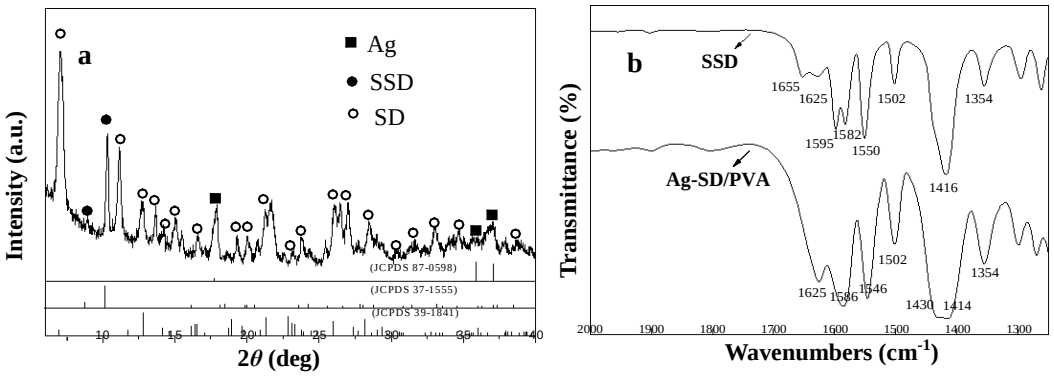

Fig. 1 (a) XRD pattern of Ag-SD/PVA NRs; (b) FTIR spectra of Ag-SD/PVA NRs and SSD MRs.

(JCPDS 39-1841), respectively. At the same time, the peaks at 2θ of 17.7°, 35.9° and 37.0° are ascribed to Ag crystal planes of (002), (004) and (101) (JCPDS 87-0598), respectively. Therefore, the sample is composed of SD and metallic sliver. In addition, the peaks at 2θ of 8.9° and 10.2° could be ascribed to (002) and (011) of monoclinic SSD (JCPDS 37-1555), due to the residue of SSD precursor.

Fig.1b gives the FTIR spectra of the samples. The absorption bands at 1586, 1502 and 1414 cm^{-1} are attributed to skeletal vibrations of phenyl and pyrimidine group of SD, respectively. Furthermore, the band at 1354 cm^{-1} belongs to the symmetrical stretching of $-SO_2$ group, which indicates the main organic component of SD. Obviously, the band at 1430 cm^{-1} is characteristic of the O-H group deformation vibration in PVA, which indicates the presence of PVA in the composite. Additionally, the band at 1546 cm^{-1} can be assigned to the shifted ring vibration of pyrimidine due to the presence of Ag^+ ions,[12] which may be from the residue of SSD in the reduction process. In comparison, the FT-IR spectrum of SSD shows different features from that of Ag-SD/PVA. The phenyl skeletal vibration band is shifted towards higher wavenumber from 1586 cm^{-1} to 1595 cm^{-1} and the C-C stretching vibrations of the aromatic ring are split (1595 and 1582 cm^{-1}). Therefore, it could be concluded that organic matrix of as-synthesized sample is mainly composed of SD instead of SSD.

The morphologies of as-synthesized Ag-SD/PVA NRs were shown in Fig.2. It can be seen that the sample exhibits bundled feature with salix leaf morphology (Fig. 2a). The bundles are further found to be composed of numbers of NRs with diameters of about 50 nm and lengths of above 300 nm (Fig 2b). To acquire more insights into the detailed microstructure of as-synthesized sample, we conducted TEM analysis of single nanorod separated from the bundle-like structure (Fig 2c). It is clear that many spherical nanoparticles are homogeneously adhered to

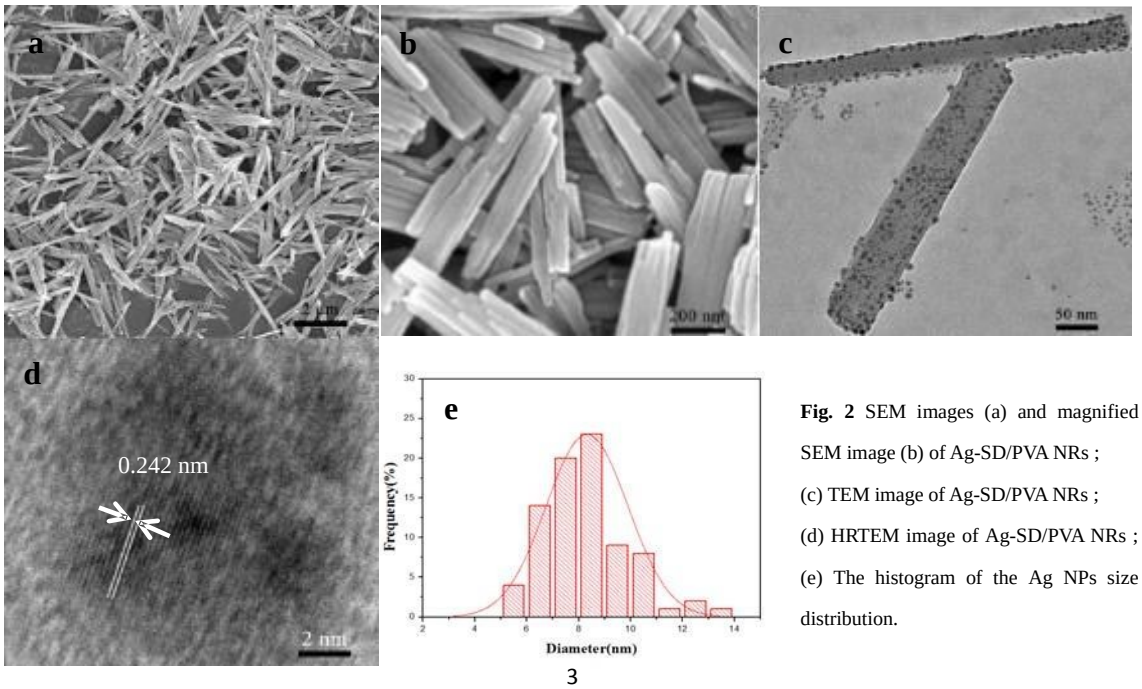

Fig. 2 SEM images (a) and magnified SEM image (b) of Ag-SD/PVA NRs ; (c) TEM image of Ag-SD/PVA NRs ; (d) HRTEM image of Ag-SD/PVA NRs ; (e) The histogram of the Ag NPs size distribution.

SD NRs. Furthermore, HRTEM image of a section of a single nanorod is shown in Fig 2d, the lattice spacing of about 0.242 nm corresponds the (101) crystal plane of Ag (JCPDS 87-0598). However, due the organic component of SD, there aren't obvious lattice spacings in the nanorod. Additionally, the size distribution of Ag NPs was shown in Fig 2e. It is obvious that Ag NPs exhibit uniform spherical shape, and have an average size of 8 nm with a size distribution of 8 ± 2.2 nm.

The possible growth mechanism of Ag-SD/PVA NRs is illustrated in Fig.3. Under the ultrasonic condition, the hydrogen bond between the hydroxyl groups of PVA chains and the amine groups of SD molecules were formed to produce SD/PVA composites. When Ag^+ ions were introduced, SSD/PVA NRs were gradually formed for the reaction between Ag^+ ions and SD. Meanwhile, Ag^+ ions on the surface of SSD/PVA NRs were reduced to Ag atoms by PVA, which led to a diffusion of the inner SSD-bound Ag^+ ions to the outer surfaces of the organic matrix and further reduction to Ag atoms.[13] Subsequently, silver atoms were agglomerated to Ag NPs and SSD/PVA NRs precursor were gradually changed into SD/PVA NRs without change of morphology due to the similar monoclinic structure of SSD and SD. Finally, Ag NPs were loaded on the surface of SD/PVA NRs through coordination bond. In the process, PVA possesses dual functions (a) as a reducing agent to reduce silver ions to elemental silver, and (b) as a steric hindrance agent to control the size of SSD NRs and Ag NPs.[14]

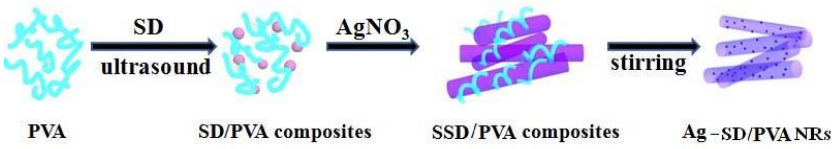

Fig. 3 Illustration of the synthetic procedure of Ag-SD /PVA NRs.

2.3 Antimicrobial assay of Ag-SD/PVA NRs.

The antimicrobial activity of Ag-SD/PVA NRs against the three tested strains of *S. aureus*, *P. aeruginosa* and *E. coli* was evaluated by MIC, MBC and inhibition zone assays. For comparison, the results of Ag NPs, SSD MRs and PVA were given. All the experiments were performed in triplicate to ensure the credible data.

Minimum inhibition concentration (MIC) and minimal bactericidal concentration (MBC) methods were applied to assess the antibacterial activity of the samples.[15,16] In the MIC test, the serial sample solutions with different concentrations were dispersed in sterilized tubes with 2 mL broth media by a two-fold serial dilution method. Then 20 μL bacteria suspensions (10^8 CFU/mL) were added into the serial tubes, respectively. Finally, the tubes were incubated at 37℃for 24 h and the lowest concentration of samples that inhibited visible growth of bacteria by turbidimetric method were signed as the MIC values.[17] Additionally, in the MBC test, the nutrient agar

was spread onto a Petri plate, and then the invisible bacterial suspensions with different concentration of samples taken out from the tubes were coated on the agar plates. Final agar plates with bacterial suspension were incubated at 37℃ for 24 h. The number of survival colonies was counted to get the MBC values of the sample.[18]

The antibacterial activity of Ag-SD/PVA NRs against tested strains was also measured by cup diffusion method.[19] The nutrient agar was first spread onto a Petri plate, and then 100 μL of bacteria suspension was coated on the agar plate. Subsequently, Oxford cups were placed on an agar plate, and 50 μL of sample solution with different concentrations was added into the cup hole. Meanwhile, 0.9% of sterilized saline was selected as contrast sample dropped into the central cups. After incubation at 37°C for 24 h, the inhibition rings were measured to evaluate the antibacterial effect.

As shown in Table 1, Ag-SD/PVA NRs exhibited excellent antibacterial performance compared to Ag NPs and SSD MRs, while PVA didn't perform antibacterial activity at all. For SSD, the MIC and MBC values of three bacterial stains were much higher than those of Ag-SD/PVA, which was possibly attributed to the poor dissolution of SSD in the media. Additionally, the MIC values for Ag and Ag-SD/PVA were equal or nearly equal, and the MBC values for Ag were much higher than that of Ag-SD/PVA. Therefore, the improved solubility of SD with small sizes and the combination of Ag with SD would contribute to the excellent antibacterial performance. Therefore, the prepared Ag-SD/PVA NRs, as new antibacterial agent showed higher bactericidal efficacy than Ag NPs and SSD MRs.

Table 1 MIC and MBC values of PVA, Ag NPs, SSD MRs and Ag-SD/PVA NRs.

	MIC(μg/mL)			**MBC(μg/mL)**		
	S.aureus	***E.coli***	***P.aeruginosa***	***S.aureus***	***E.coli***	***P.aeruginosa***
PVA	--	--	--	--	--	--
Ag	7.8	7.8	15.6	125	31.3	--
SSD	15.6	31.3	62.5	250	125	1000
Ag-SD/PVA	7.8	7.8	7.8	15.6	15.6	125

--: indicating no antibacterial properties.

Ag-SD/PVA NPs against three strains of *S. aureus*, *P. aeruginosa* and *E. coli* were further measured by cup diffusion method (Fig. 4). Here, the concentrations of Ag-SD/PVA sample were 2000 μg/mL, 1000 μg/mL, 500 μg/mL, 250 μg/mL, 125 μg/mL, 62.5 μg/mL, 31.25 μg/mL, 15.62 μg/mL, corresponding to the number from one to eight, and the control group in the middle was 0.9% normal saline. In Fig.4a, after incubation at 37℃ for 24h,

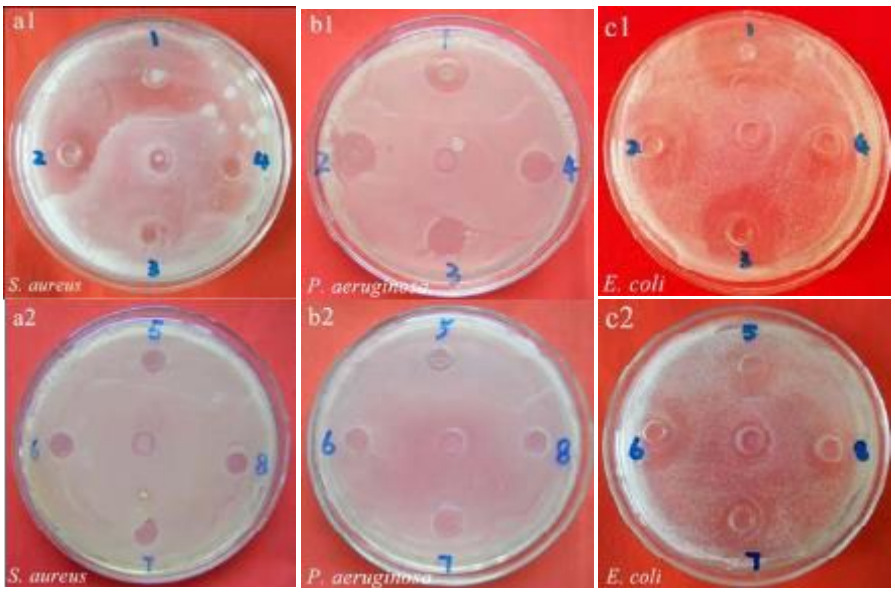

Fig. 4 Inhibition zone photographs of Ag-SD/PVA NRs against bacteria *S. aureus* (a1, a2), *P. aeruginosa* (b1, b2) and *E. coli* (c1, c2). (1–8) Samples correspond concentrations with 2000, 1000, 500, 250, 125, 62.5, 31.25, 15.62 μg/mL and the control group in the middle is 9% normal saline.

Ag-SD/PVA hardly displayed antibacterial activity towards *S. aureus* below the concentration of 500 μg/mL. However, when the concentration was increased to 1000 μg/mL or more, the diameter of inhibition zones were obviously enhanced. To *P. aeruginosa*, when the sample concentration was raised to 250 μg/mL, the antibacterial activity was gradually displayed as the diameter of inhibition zone increased (Fig.4b). As shown in Fig.4c, to *E. coli*, the diameter of inhibition zones was always increased when the concentrations varied from low to high. Therefore, the experiments indicated that the obtained Ag-SD/PVA NRs displayed more sensitive towards *S. aureus* than *P. aeruginosa* and *E. coli* at higher concentrations, and exhibited more sensitive towards *E. coli* than *S. aureus* and *P. aeruginosa* at lower concentrations, which was possibly due to the synergistic antibacterial activities of Ag NPs and SD NRs, or the difference in the structure of the cell wall between gram-negative and gram-positive bacteria. The interest results would be worth further studying in the future work.

4. Conclusions

Ag-SD/PVA NRs were successfully fabricated in an ammonia solution, with typical morphology of Ag NPs loaded on the surface of SD/PVA NRs. The possible forming mechanism was proposed that SSD/PVA NRs precursor were reduced by PVA to produce Ag-SD/PVA NRs. Antibacterial activity experiments showed that Ag-SD/PVA NRs, as new composite antibacterial agents, exhibited higher bactericidal efficacy than that of Ag NPs and SSD MRs alone. Furthermore, Ag-SD/PVA NRs displayed more antibacterial sensitive towards *S. aureus*

than *P. aeruginosa* and *E. coli* at higher concentrations, and exhibited more sensitive towards *E. coli* than *S. aureus* and *P. aeruginosa* at lower concentrations. The reason may be the synergistic bactericidal activity of Ag NPs and SD NRs, or the difference in the structure of the cell wall between gram-negative and gram-positive bacteria.

Acknowledgment

Financial support of this work from National Natural Science Foundation of China (21271062), Foundation of Science and Technology of Henan Province (14B150003)

References

1 P.N. Kalaria, J.A. Makawana, S. P. Satasia, D.K. Raval and H. Zhu, *Chem. Commun.*, 2014, 5, 1555-1562

2 A. Zablotskaya, I. Segal, A. Geronikaki, G. Kazachonokh,Y. Popelis, I. Shestakova, V. Nikolajeva and D.Eze, *Chem. Commun.*, 2015, view article online.

3 B. Li, Y. Li, Y. Wu and Y. Zhao, *Mater. Sci. Eng. C*, 2014, **35**, 205-211.

4 A. Dong, S. Lan, J. Huang, T. Wang, T. Zhao, L. Xiao, W. Wang, X. Zheng, F. Liu, G. Gao and Y. Chen, *ACS Appl. Mater. Interfaces*, 2011,**3**, 4228-4235.

5 J. R. Morones, J. L. Elechiguerra, A. Camacho, K. Holt, J.B. Kouri, J.T. Ramirez and M.J. Yacaman, *Nanotechnology*, 2005,**16**,2346-2353.

6 N.Iqbal, M. R.A. Kadir, N.A.N.N.Malek, N. H. Mahmooda, M. R. Murali and T. Kamarul, *Mater. Lett.*, 2012 **89**,118-122

7 M. J. Prieto, D. Bacigalupe, O. Pardini, J.I. Amalvy, C. Venturini, M.J. Morilla and E.L. Romero, *Int. J. Pharm*. 2006, **326**, 160-168.

8 J. Nesamony and W.Kolling, *J. Pharm. Sci.*, 2005, **94**, 1310-1320

9 H.Kong and .J. Jang, *Langmuir*, 2008, **24**, 2051-2056.

10 J. Song, H. Kong and J. Jang, *Colloids Surf B Biointerfaces*, 2011,**82**, 651-656.

11 M. Zasloff, *Nature*, 2002, **415**, 389-395.

12 A. Szegedi, M. Popova, K. Yoncheva, J. Makk, J. Mihaly, and P. Shestakova. *J. Mater. Chem. B*, 2014, **2** 6283-6292

13 H. Kong, J. Song and J. Jang, *Macromol Rapid Commun*, 2009, **30**, 1350-1355.

14 R. Bryaskova, D. Pencheva, G. M. Kale, U. Lad and T. Kantardjiev, *J. Colloid. Interf. Sci.*, 2010, 349, 77-85

15 S.Imazato, A.Kuramoto ,T.Kaneko ,S. Ebisu and R.R. Russell，*Am. J.Dent.*, 2002, 15,356-60 16

F.Rehman, M. Sudhaker, S.Roshan and A. Khan, *Pharmacognosy Journal*, 2012, 4, 67-70

17 A-T.Le, L-T.Tam, P.D. Tam, P.T Huy, T.Q. Huy, N.V.Hieu, A.A.Kudrinskiy and, Y.A.Krutyakov, *Mater. Sci. Eng. C*, 2010, 30, 910-916

18 A. Zablotskaya, I. Segal, A.Geronikaki, G. Kazachonokh, Y. Popelis, I.Shestakova, V. Nikolajeva and D. Eze, *Med. Chem. Commun.*, 2015, 6, 1464-1470

19 Z. Ni, Z.Wang, L. Sun, B. Li and Y, Zhao, *Mater. Sci. Eng. C*, 2014, 41, 249-254